# High-Resolution Adsorption Isotherms of Supercritical Carbon Dioxide on Activated Carbon

**Raashina Humayun and David L. Tomasko**
Dept. of Chemical Engineering, The Ohio State University, 140 W. 19th Ave., Columbus, OH 43210

*Supercritical fluids are attractive solvents for heterogeneous processes, including catalysis and adsorptive separation. However, adsorption processes in the near-critical region are poorly understood and exhibit unique behavior where the adsorption of the supercritical solvent plays an important role in the solute adsorption. The behavior of supercritical fluids in confined pores has been studied theoretically, but there are few experimental data on their behavior in industrially important microporous materials. The adsorption of carbon dioxide on Calgon F400 activated carbon over a wide range of pressures (0–20 MPa) at temperatures near the critical point of carbon dioxide (30 to 45°C) was studied. Near-continuous adsorption and desorption isotherms were measured with a new flow gravimetric apparatus with precise control over pressure and temperature. As pressure is increased, the excess adsorption increases sharply at low pressures; then a broad maximum is observed. At temperatures greater than the critical temperature, there is a sharp drop in excess adsorption near the critical region where the density of the bulk fluid increases sharply. A crossover is observed near the critical region where, below a certain pressure, the excess adsorption decreases with temperature, while above the crossover point the trend is reversed. When analyzed as a function of solvent density, the crossover disappears, revealing an anomalous maximum in total adsorption near the critical point similar to the enhanced local density or ''charisma'' observed in binary solute–supercritical fluid systems. A 2-D EOS model using the 2-D Peng-Robinson EOS was able to qualitatively describe the adsorption behavior over the entire pressure range, but the quantitative agreement was poor in the near-critical region.*

## Introduction

In recent years supercritical fluids (SCFs), specifically supercritical carbon dioxide (SC-$CO_2$), have received much attention as environmentally benign solvents and have been applied in various fields (McHugh and Krukonis, 1993). The favorable mass-transfer properties, due to their low viscosity and the absence of solvent residue problems, make SCFs especially attractive solvents for heterogeneous processes in which surface transport and adsorption–desorption steps are important. Examples of such processes include extraction from solid matrices, regeneration of adsorbents, SCF chromatography, adsorptive separations, and heterogeneous catalysis. It is now being recognized that the SC-solvent plays an important role in adsorptive processes (King, 1987), and that the interaction between SCF and the solid surfaces and its effect on the solute adsorption should not be ignored (Chen et al., 1997). However, it has been common practice to treat the supercritical solvent as a continuum, with solutes simply partitioning between the surface and the fluid. This is an oversimplified approach, as there is a significant adsorption of the solvent and the system is essentially multicomponent. In order to better understand heterogeneous processes involving supercritical fluids, it is imperative to obtain information about the adsorption–desorption behavior. Most researchers in the field point to the paucity and need for accurate SCF adsorption isotherm data for systems of practical interest.

Correspondence concerning this article should be addressed to D. L. Tomasko.

High-pressure adsorption studies by Findenegg and coworkers on nonporous graphite and controlled pore glass (Specovius and Findenegg, 1980; Findenegg, 1983; Thommes et al., 1994) revealed some interesting aspects of adsorption in the near-critical region. For adsorption above the critical temperature ($T_c$) on nonporous homogeneous high-energy surfaces the surface excess isotherms generally pass through a sharp maximum, beyond which the surface excess amount decreases. Below $T_c$, as the partial pressure approaches the saturation pressure ($P_{sat}$) of the bulk fluid, excess adsorption increases until $P_{sat}$, where there is a discontinuity in the isotherm as the bulk fluid condenses. At very high temperatures the adsorption resembles gaseous phase adsorption.

In the region close to the critical point, the compressibility of the bulk fluid becomes very large. Small perturbations to the intermolecular forces brought about by the presence of an attractive solute lead to large enhancements in the local density around that solute, as observed by many different techniques (Brennecke et al., 1990; Eckert and Knutson, 1993; O'Brien et al., 1993; Tucker and Maddox, 1998). On a molecular level there may be similarities between fluid-phase solvent–solute interactions and fluid–solid interactions in physical adsorption (Subramanian et al., 1995). Findenegg's results for the adsorption of ethylene on graphitized carbon black (Specovius and Findenegg, 1980) indicate that the density profile in the interfacial region of a supercritical fluid near an adsorbing surface, becomes long range as the critical point is approached. In microporous materials commonly used in engineering applications, the depth of the density profile is limited by the pore size. In addition, pore geometry and pore-size distribution, as well as surface heterogeneity in materials like activated carbon, also affect the adsorption behavior.

The region very close to the critical point has been the subject of several recent studies. There is considerable debate about the fundamental thermodynamics and kinetics behind near-critical adsorption effects including critical depletion (Thommes et al., 1994) and pore critical temperature (Michalski et al., 1991; Morishige and Shikimi, 1998; Machin, 1999).

An understanding of the physical adsorption of gases and knowledge of the structure and thermodynamics of compressed gas/solid interfaces is fundamental to the successful development of separation and reaction processes involving SCF–solid interactions. This complex nature of adsorptive processes in the near-critical region points to the need to study pure solvent adsorption as a first step toward understanding multicomponent (SCF + one or more solutes) adsorption that would govern SCF heterogeneous processes. However, there is little experimental data for near-critical adsorption in systems of practical interest (Jones et al., 1959; Ozawa et al., 1975; Wakasugi et al., 1981; Strubinger and Parcher, 1989; Chen et al., 1997).

This article reports the results of our investigation of the adsorption behavior of supercritical carbon dioxide on a common microporous adsorbent–activated carbon. Accurate adsorption–desorption isotherms were measured using a high-pressure flow gravimetric apparatus. While earlier researchers favored the use of volumetric methods and expressed concern over the certainty of gravimetric measurements at high pressures (Menon, 1968), recent improvements in high-pressure microbalances with accurate temperature and pressure-control mechanisms have resulted in their increased application in high-pressure research (Sahle-Demessie et al., 1998; Weireld et al., 1999). Sircar (1999) provides a review of current adsorption methods.

The objective of this research is to understand the adsorption of supercritical fluids and aid in the development of experimental and modeling procedures that would account for solvent adsorption. The high-resolution isotherms presented here will provide a much more stringent test of adsorption models—particularly in the near-critical region—than traditional isotherms containing several discrete points. They would also allow single-solute adsorption to be treated as a multicomponent process, with the adsorption of both solute and solvent being taken into account.

While solubilities in supercritical fluids can be calculated easily with sophisticated equations of state (Brennecke and Eckert, 1989; Johnston et al., 1989), SCF adsorptive studies, due to lack of adsorption isotherm data, commonly rely on kinetic or simplified equilibrium models to describe the adsorption behavior. Unfortunately, because these systems often involve a nonideal SCF solution interacting with a highly complex surface, these correlations are not very general and cannot predict behavior for other surfaces or solutes. A significant difficulty encountered when considering supercritical adsorption processes is that, in addition to fluid-phase solute concentration, both the system temperature and the density of the supercritical fluid influence the adsorption equilibria (Tan and Liou, 1990; Kikik et al., 1996). This phenomenon complicates commonly used adsorption models (e.g., Langmuir and Freundlich) that have to be modified to include a density dependence of the parameters (Kikik et al., 1996).

Over the past decade there have been major advances in the application of molecular simulation and statistical mechanical methods to the study of adsorption (Afrane and Chimowitz, 1993; Aranovich and Donohue, 1996; Gubbins, 1997). However, these techniques can be computationally intensive. Simple models that can bridge the gap between complex statistical–mechanical models and overly simple empirical models are useful for engineering design. A frequently used approach is to treat the adsorbed molecules as a separate phase subject to classic thermodynamic principles. The adsorbed solution theory and two-dimensional (2-D) equation-of-state models (2-D–EOS) are based on this approach. The advantage of such models lies in the fact that they are computationally simple and lend themselves to thermodynamic analysis. It is thus possible to extend the models from systems where data are available (e.g., single-component systems) to other related or more complex systems (e.g., mixtures) by using mixing rules or group contribution techniques.

In this article we have evaluated the use of a 2-D–EOS model to correlate our data. Several researchers have used 2-D–EOS-based models to describe pure and multicomponent adsorption behavior on various substrates including silica gel (Haydel and Kobayashi, 1968), charcoal (Payne et al., 1968), activated carbon (Hoori and Prauznitz, 1967; DeGance, 1992; Zhou et al., 1994), and molecular sieves (Zhou et al., 1994). If such a model can accurately describe supercritical adsorption behavior, it would provide a relatively simple approach that maintains the flexibility of an EOS for extension to mixtures. Based on pure-component behavior both

for the fluid and the adsorbed phases and by using mixing rules it would be possible to predict multicomponent adsorption behavior that is intrinsic in various heterogeneous processes with supercritical fluids.

## Experimental

### *Materials*

The activated carbon (Filtrasorb-400, 12×40 mesh, Calgon Carbon) was washed in demineralized water and dried under vacuum at 110°C for 3 days before being used in adsorption experiments. The BET surface area as determined by $N_2$ adsorption at 77 K was 850 $m^2/g$ (Quantachrome Autosorb). The total pore volume for pores less than 1,200 Å was 0.66 $cm^3/g$ and the average pore radius was 17 Å. The micropores accounted for 700 $m^2/g$ with a volume of 0.37 $cm^3/g$. The sample size was 0.223 g. We acknowledge that the surface area available to $CO_2$ may be different from that measured by $N_2$ adsorption; however, as this is the most commonly reported method, we present the data here for comparison. A similar analysis for the GAC after the $CO_2$ adsorption–desorption experiments revealed no measurable difference in the carbon after exposure to $CO_2$ at high pressure.

Bone-dry carbon dioxide (99.9% liquid carbonic) was passed through a 0.5-$\mu$m filter preceded by a packed bed of activated carbon before use in adsorption experiments. Helium, pretreated in a similar manner, was used for buoyancy measurements.

### *Gravimetric adsorption apparatus*

Adsorption isotherms were measured with a high-pressure flow gravimetric apparatus developed in our laboratory (Jwayyed et al., 1997) and used previously to measure dynamic SFE data. The apparatus was modified slightly to obtain adsorption data. The experimental setup is shown in Figure 1; details not included here are available elsewhere (Jwayyed et al., 1997). The major components of the apparatus include a microbalance (Cahn 1100, 1-$\mu$g maximum sensitivity) in a stainless-steel high-pressure housing (3000 psi maximum pressure), and feed and exit pumps (ISCO 500D). The balance and housing stand on an active air vibration isolation table, and the whole system is placed inside a constant-temperature oven (Lunair, ±0.1°C). Temperature is measured by a thermistor (Omega, ±0.01°C) attached to the bottom of the sample hang-down tube. Pressure is measured by a digital pressure gauge (Sensotec, ±0.036%) attached to the microbalance housing. A data-acquisition board (Keithley Metrabyte DAS 1600) was used to continuously monitor the pressure and microbalance output. The oven is turned on and the temperature is allowed to stabilize for 2 days prior to any data collection. A single adsorption–desorption isotherm was measured over a period of 10–14 days. The pressure was measured with a certainty of ±1 psi, while temperature at the sample tube was controlled to within ±0.05°C. Over the period of operation, the maximum variation in the pressure was ±3 psi, and that for temperature was ±0.2°C. A detailed investigation of the spatial temperature gradients in the constant temperature oven showed that the maximum variation of temperature was 0.3°C and that the maximum variation of temperature in the balance housing was 0.05°C. Since the pressure was controlled independently by the pumps and due to the large heat capacity of the system, minor, short-term variations in temperature were not as critical as for volumetric isothermal or isochoric experiments.

The solid adsorbent is placed in a sample holder on one arm of the microbalance while tare weights are loaded on the other arm. Care is taken to keep the volume of the sample

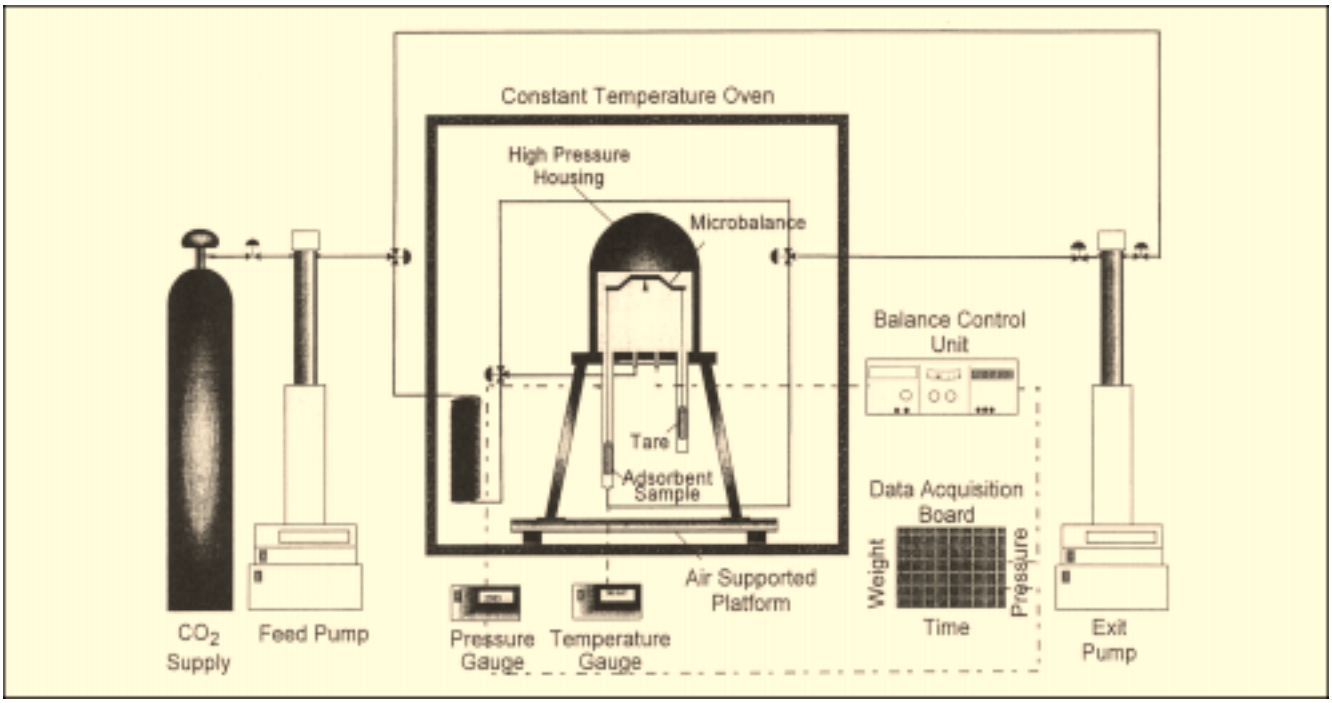


**Figure 1. Adsorption apparatus.**

and the tare side as close as possible (by using a combination of stainless-steel and glass beads) to reduce buoyancy effects. Before the start of the experiment, the system is evacuated with a vacuum pump and the balance is zeroed. Buoyancy is measured by introducing helium and pressurizing up to 20 MPa. It is assumed that helium does not adsorb, and any weight change ($\Delta M$) is due to buoyancy. Although some researchers point to the possibility of errors due to the finite adsorption of helium at high pressure (Sircar, 1999), we believe it would be negligible compared to the high level of $CO_2$ adsorption. Knowing the density ($\rho$) of helium, we can determine the difference in volume ($\Delta V$) between the sample and the tare sides according to Eq. 1:

$$\Delta V = \frac{\Delta M}{\rho_{\mathrm{He}}(P,T)}. \tag{1}$$

The measured weight can then be corrected for buoyancy effects at any temperature and pressure (Eq. 2).

$$M = M_{\mathrm{exp}} - \Delta V \rho_{\mathrm{CO_2}}(P,T). \tag{2}$$

For the data reported in this article the measured $\Delta V$ was $-0.01$ cm$^3$. The buoyancy correction in the region close to the critical point ($\rho_{\mathrm{CO_2}} \cong 12$ mol/L) was less than 3%. At the highest pressure where the density was maximum ($\rho_{\mathrm{CO_2}} \cong 20$ mol/L) and the surface excess was low, the buoyancy correction was less than 20%.

After the buoyancy measurement the system is evacuated again and $CO_2$ is introduced by slowly opening a metering valve. After the balance is at the initial pump pressure, an electronically controlled pressure program is initiated where the pressure is raised at a predetermined rate (0.1 to 1.2 MPa/h) for 10–20 min, held at a constant pressure for 5–10 min, and then raised again. At all times the fluid flow rate is small enough ($< 2$ mL/min at experimental conditions), so hydrodynamic drag can be neglected (Jwayyed et al., 1997). The fluid delivered to the microbalance comes in contact with the adsorbent and the excess adsorption, measured as an increase in weight by the balance, is continuously recorded by a computer. Thus, as the pressure is incrementally increased from 0 to 20 MPa, a continuous adsorption isotherm can be obtained. Similarly, desorption isotherms are measured by using the exit pump to draw fluid out of the system at a controlled rate. A vacuum pump is used to evacuate the system below atmospheric pressure. Isotherms at different temperatures were measured for the same adsorbent sample. The BET analysis conducted on the GAC before and after the experiments indicated no measurable change in pore structure.

With the dynamic ability of the flow gravimetric system, continuous adsorption and desorption isotherms are obtained by increasing and decreasing the pressure at a very slow rate so the system is at equilibrium. Equilibrium conditions were verified when the desorption isotherm followed the adsorption isotherm, since in these two steps the equilibrium is approached from opposite sides. In addition, the rate of change of pressure was also varied to confirm the absence of kinetic or mass-transfer effects. These effects were negligible at all conditions studied, with the possible exception (discussed below) of the regions of very high compressibility.

One limitation of the system is that, due to the large volume of the apparatus, it requires a finite amount of time to induce large changes, such as condensation or evaporation. For example, when the saturation pressure is reached all the fluid does not condense spontaneously, but does so over several minutes as enough $CO_2$ is introduced into the system to account for the change in density. Similarly, below $T_c$ as the pressure is decreased, there is a lot of noise at the saturation pressure as the $CO_2$ starts to evaporate and the relative weights of the sample and the tare sides go up and down as drops evaporate from each.

It is important to point out that the total adsorption cannot be directly measured and the quantity measured in our experiments is the Gibb's surface excess ($\Gamma^{\mathrm{excess}}$). For a flat surface, $\Gamma^{\mathrm{excess}}$ can be defined as in Eq. 3, where $z$ is the distance from the solid surface and $\rho$ is the density of the adsorbate.

$$\Gamma^{\mathrm{excess}} = \int_0^{\infty} [\,\rho(z) - \rho_{\mathrm{bulk}}\,]\, dz. \tag{3}$$

For porous adsorbents the exact definition would require integration to the center of the pore with appropriate coordinates; however, by placing the Gibb's dividing surface arbitrarily in the bulk fluid phase (Sircar, 1999), the excess is described as a summation for all the pores.

### *Data rectification*

The continuous pressure vs. weight data is further rectified to reduce electronic and vibrational noise. A MATLAB program based on multiscale Univariate filtering that uses a wavelet thresholding approach (Donoho et al., 1995; Bakshi et al., 1997) was used to reduce noise from the pressure vs. weight data. This procedure for rectification of random errors is based on representing the measured variables at multiple scales by decomposition on time frequency localized basis functions derived from orthonormal wavelets. This method provides better rectification than that by the widely used method of exponential smoothing.

## Results and Discussion

### *Adsorption isotherms*

The adsorption/desorption isotherms at 30.5, 32, 36, 40 and 45°C are shown in Figures 2a–2e. Surface excess and bulk fluid density are shown vs. pressure at each temperature. Each point on the plot refers to a one-in-ten sampling of the raw data after rectification and buoyancy correction; sequential points were collected at an interval of 50 s or more. Any gaps indicate data lost during data acquisition. Also included in Figure 2 is previously published adsorption data for $CO_2$ on activated carbon. Ozawa et al. (1975) reported adsorption isotherms (desorption was not reported) for five different types of activated carbon at temperatures from 40°C to 80°C and pressures up to 17 MPa. Chen et al. (1997) reported adsorption–desorption isotherms for Degussa IV carbon from 298 K to 323 K and pressures up to 14 MPa. Our data are compared with those of Chen et al. at four similar tempera-

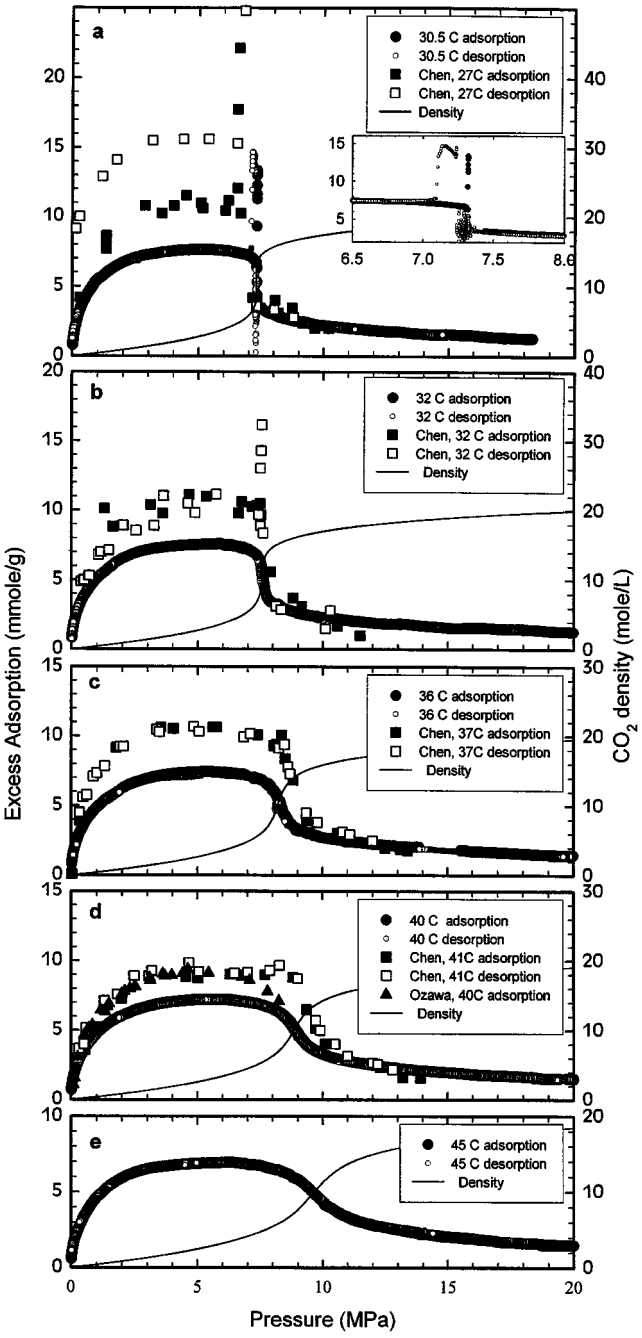


**Figure 2. Adsorption–desorption isotherms of $CO_2$ on GAC at (a) 30.5, (b) 32, (c) 36, (d) 40, (e) 45°C; density is plotted on the righthand axis.**

The inset in part (a) shows the condensation and hysteresis at $P_{sat}$. Also shown are previously published data (Ozawa et al., 1975; Chen et al., 1997) at similar (but not identical) conditions.

tures (27, 32, 36 and 41°C) and with Ozawa's data at 40°C. The continuous-flow gravimetric technique coupled with wavelet rectification allows a higher precision, especially in the near-critical region than the volumetric technique used by previous researchers.

Just below the critical point at 30.5°C (Figure 2a), the excess adsorption increases sharply with pressure at low pressures. As the pressure approaches 1 MPa, the isotherm starts to level off and we observe a broad maxima below the saturation pressure ($P_{sat}$). As $P_{sat}$ is approached, the gas condenses first in the pores and the weight of the adsorbent increases sharply, as shown by the discontinuity in the adsorption isotherm in Figure 2a. When condensation is complete, the excess adsorption drops sharply and continues to decrease, as the molecules in the adsorbed layer are in equilibrium with liquid $CO_2$. It should be noted here that even when the bulk fluid is liquid, there is a finite amount of excess adsorption indicating that at the same temperature and pressure, the density of the adsorbed phase is greater than that of liquid $CO_2$. Desorption follows the adsorption isotherm closely, although there appears to be a slight hysteresis at the saturation pressure when the fluid in the pores remains in the liquid state until the pressure is approximately 0.2 MPa lower than the bulk saturation pressure. The order of magnitude of the hysteresis is in agreement with the Kelvin effect (Gregg and Sing, 1967); however, it might also be in part due to a nonequilibrium effect. Comparing with the subcritical adsorption–desorption isotherm from Chen et al. (1997), (our data at 30.5°C, $T_r = 0.998$; Chen's data at 27°C, $T_r = 0.988$) we note that both adsorption isotherms show a discontinuity at the saturation pressure, followed by a sharp drop in excess adsorption as the bulk fluid becomes liquid. However, Chen's desorption isotherm shows a large hysteresis loop where the subsaturation surface excess was approximately 50% higher during desorption even as the pressure approached 0 MPa. Our data, which are much closer to the critical point, do not show this large hysteresis effect. The reason for this is not clear; however, Chen's isotherm is at a lower reduced temperature ($T_r = 0.988$) compared to our isotherm ($T_r = 0.999$), and different types of activated carbon were used in the two studies. The carbon used by Chen et al. had a much higher surface area (1,600 $m^2/g$ vs. 850 $m^2/g$) with a much higher micropore volume. A smaller pore size would result in a larger hysteresis due to the Kelvin effect as well as greater mass-transfer effects.

The remaining isotherms were measured above the critical temperature (Figures 2b–2e). At temperatures greater than the critical temperature of the fluid (31°C) the adsorption isotherms also show a sharp slope at low pressure, which then levels off as pressure is increased. All isotherms go through a broad maximum, but the drop in excess adsorption near the critical point is continuous, as there is no phase change or condensation. The density of the bulk fluid rises sharply but continuously near the critical point, and the excess adsorption drops because the rate of increase of adsorbed phase density is less than that of the fluid. Sufficiently far from the critical point, where the bulk fluid becomes relatively incompressible, the surface excess also levels off somewhat, though it still continues to decrease almost linearly. The desorption isotherm closely follows the adsorption isotherm (within the limits of experimental error) for the major part of the experiment. In the region near the critical point where the excess adsorption changes sharply, there appears to be a slight hysteresis at the lower temperatures. However, the heights of the maxima in all isotherms is the same for both adsorption and desorption. This may be indicative of possible mass-transfer effects in the region where the bulk fluid density and the adsorption amount change very rapidly. The general shape

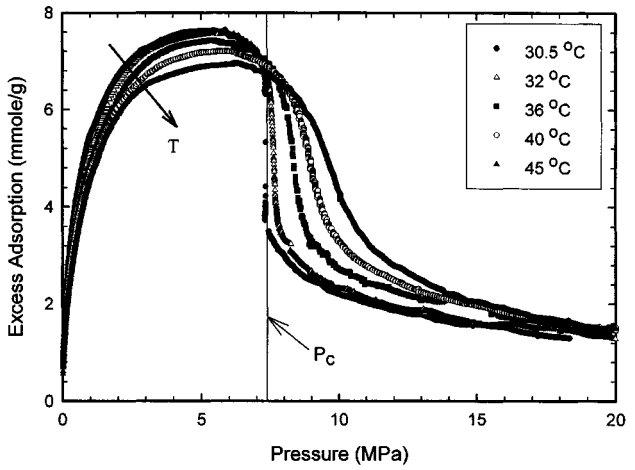


**Figure 3. Adsorption isotherms of $CO_2$ on GAC showing the crossover near the critical point.**

of the isotherms is similar to those of Chen et al. (1997) and Ozawa et al. (1975) except at 32°C. At this temperature Chen's data show a sharp spike near the critical pressure, which is indicative of condensation in the pores even though the bulk fluid was supercritical. This effect cannot be attributed to the pore-critical behavior, since studies on mesoporous-controlled pore glass (Machin, 1999) and mesoporous graphitic carbon (Michalski et al., 1991) have shown that the critical temperature in small pores is lowered so that condensation does not occur even at temperatures slightly below the bulk-critical temperature. Chen's desorption isotherm also did not show any hysteresis, indicating a phenomenon different from condensation. Our data show a continuous transition from bulk gaseous to supercritical conditions at this temperature without any pore condensation. It is possible that the discontinuity in Chen's data is actually an artifact due to the volumetric measurement technique since it requires a conversion of pressure and volume data into moles. Since both the density and the surface excess change very sharply near the critical point, very small errors in either the pressure or temperature measurements could cause this observed "spike." Chen's data show this aberration at 37 and 41°C to lesser degrees. At 40°C the shape of our isotherm is qualitatively similar to those of Ozawa and Chen (41°C).

Figure 3 shows the five adsorption isotherms plotted together to highlight the crossover phenomenon. At lower pressures, as the critical temperature is approached (i.e., from 45°C to 32°C), the maxima becomes sharper and higher while the drop in surface excess near the critical point becomes steeper and larger, resulting in a crossover near the critical point. Thus at a lower temperature the maximum surface excess is greater, but the surface excess after the crossover point is lower. This crossover in the SC-solvent adsorption isotherms may have interesting implications for the adsorption of solutes from supercritical solutions and may explain similar crossover behavior observed for the adsorption of toluene from SC-$CO_2$ onto activated carbon (Tan and Liou, 1990), as demonstrated in Figure 4.

## Thermodynamic Analysis and Modeling

### *Total adsorption from Gibbsian excess*

In high-pressure adsorption, a major challenge in applying most modeling procedures and further thermodynamic analysis is to estimate the total adsorption from the excess adsorption data. This fact is often ignored in gas-adsorption studies, as the density of the bulk phase is very small compared to the adsorbed phase density and the difference between total adsorption and excess adsorption is negligibly small. For high-pressure adsorption, however, when the density of the bulk fluid becomes significant, the shape of the excess isotherm is strongly dependent on the bulk density and the total adsorption is significantly higher than the excess.

In order to estimate the total adsorption we need to determine either the density or the volume of the adsorbed phase, and several assumptions have been used in the literature to carry this out. A common assumption (Sircar and Myers, 1971) is that the adsorbed phase density is equal to the liquid density, that is, a pure liquid in equilibrium with a solid surface would have a zero surface excess. This is not valid at least for the carbon-dioxide-activated carbon system, where a signifi-

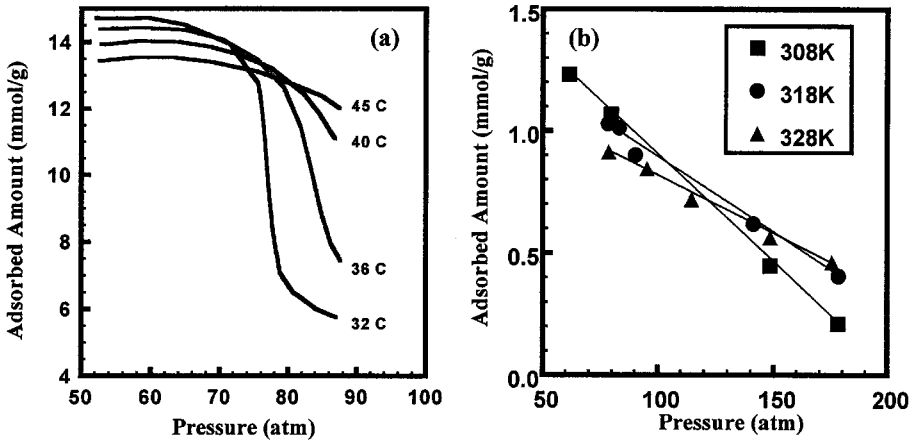


**Figure 4. Crossover in supercritical fluid adsorption on activated carbon.**

(a) Adsorption of pure $CO_2$; (b) adsorption of toluene from SC-$CO_2$ (Tan and Liou, 1990).

cant surface excess was observed beyond the saturation pressure (Figure 2a) when the surface was in equilibrium with liquid $CO_2$, indicating that the density of the adsorbed phase is greater than the liquid density at the same temperature and pressure. Other assumptions regarding the density of the adsorbed phase include close packing of molecules at a specified diameter, usually corresponding to the van der Waals volume (DeGance, 1992). Haydel and Kobayashi (1967) experimentally determined the adsorbed phase density for methane and propane on silica gel and found it to be close to the inverse of the van der Waals volume of the adsorbate. Another method is to determine the volume or thickness of the adsorbed phase. It is often assumed that all the fluid inside the pores of the adsorbent could be considered to be adsorbed, that is, that the pore volume was equal to the adsorbed phase volume (Wakasugi et al., 1981; Salem et al., 1998). Another method to estimate adsorption volume is to assign a thickness to the adsorbed phase equal to the range of the effective potential into the fluid phase (Payne et al., 1968). Often this thickness is based on a model like the Lennard-Jones potential. One might also assume the adsorption to be monolayer, and determine total adsorption based on the size of the adsorbate molecule and the surface area of the adsorbent. Matters are complicated for heterogeneous microporous materials like activated carbon where pore geometry and pore-size distributions coupled with the difficulty in the measurement of pore volumes and surface area can impose limitations to any of the preceding assumptions.

Because the pressure dependence of the surface excess includes the compressibility of the fluid phase, it is difficult to interpret supercritical adsorption isotherms, as shown in Figure 3. It is more meaningful to plot adsorption as a function of density. Figure 5 shows the isotherms at the five temperatures plotted vs. fluid density. The fluid density was calculated using a modified BWR EOS (Jacobsen and Stewart, 1973; Ely et al., 1989). The shape of the $\Gamma^{excess}$ vs. $\rho$ isotherms shows a sharp rise at low densities followed by a maximum at fairly low densities (2–4 mol/L). As the density increases at higher temperatures, especially at 45°C, the excess decreases almost linearly with density. At temperatures closer to $T_c$,

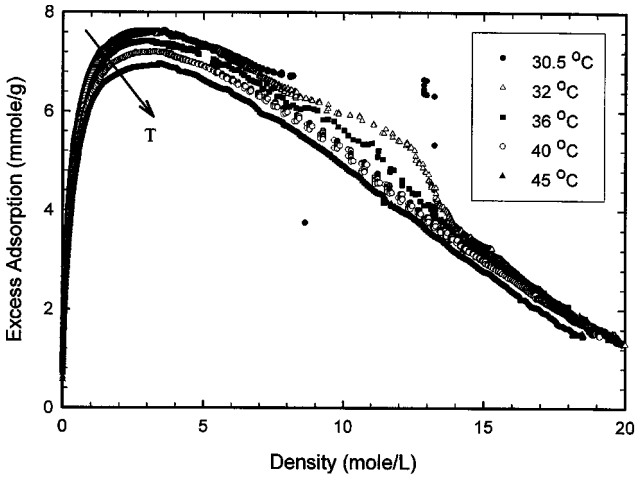


**Figure 5. Adsorption isotherms of $CO_2$ on GAC plotted as a function of bulk fluid density.**

**Table 1. Adsorbed Phase Properties Calculated from High-Pressure Adsorption Data**

| Temp. (°C) | Vol. ($cm^3/g$) | Dens. (mmol/$cm^3$) |
|---|---|---|
| 30.5 | 0.362 | 23.50 |
| 32 | 0.355 | 23.60 |
| 36 | 0.363 | 23.47 |
| 40 | 0.356 | 23.22 |
| 45 | 0.364 | 22.93 |
| Saturated liquid at 30.5°C: | | 12.78 |
| Liquid density at 20 MPa and 30.5°C: | | 20.19 |
| Density corresponding to van der Waals vol.: | | 23.45 |

$\Gamma^{excess}$ appears to rise again as the critical density is approached. However, after a certain point $\Gamma^{excess}$ drops again and becomes linear. Let us first focus attention on the linear portion at high densities. At high pressure ($>15$ Mpa) the excess adsorption is linear vs. bulk density for all temperatures. If the adsorbed phase extends to a finite distance beyond the surface, then the surface excess can be written in terms of the adsorbed phase density and volume as

$$\Gamma^{excess} = \rho^{ads} V^{ads} - \rho^{f} V^{ads}. \quad (4)$$

The linear relationship between $\Gamma^{excess}$ and $\rho^f$ at high densities indicates that after a certain point the adsorbed phase density and volume become constant. The slope and intercept would give the density and the volume of the adsorbed phase. Table 1 lists the volume and density of the adsorbed phase as calculated in this manner. The volume of the absorbed phase is constant in the temperature range of the experiments, and the density of the adsorbed phase, though varying slightly with temperature (decreasing with increasing temperature), is close to the density corresponding to the van der Waals volume of carbon dioxide. This is consistent with reports in the literature regarding the density of the adsorbed phase (Haydel and Kobayashi, 1967). This information provides us with a means of estimating the total adsorption from excess adsorption data. It is interesting to note that this adsorbed phase volume (0.36 $cm^3/g$) is significantly less than the total pore volume of the activated carbon (0.66 $cm^3/g$). Assuming that the volume of the adsorbed phase can be considered to be constant over the temperature and pressure range of our experiments, we have estimated the total adsorption based on an adsorbed phase volume of 0.36 $cm^3/g$. By using this method of directly estimating the adsorbed phase volume, we do not have to rely on surface-area measurements, which are often inconsistent. Similar approaches based on high-pressure adsorption data have been used previously to estimate adsorbed phase properties (Menon, 1968) as well as adsorbent surface area (Aranovich and Donohue, 1997a). The results of our analysis are plotted in Figure 6. It appears that the total adsorption isotherms are similar for the most part to type 1 isotherms of Brauer's classification, indicating adsorption in a single layer that gets ''filled'' as the pressure is increased until after a certain point where the total adsorption becomes constant, indicating a saturation of the monolayer. All the isotherms still show a subtle maximum at low density, however, which contradicts the expected behavior for total adsorption (i.e., monotonically increasing).

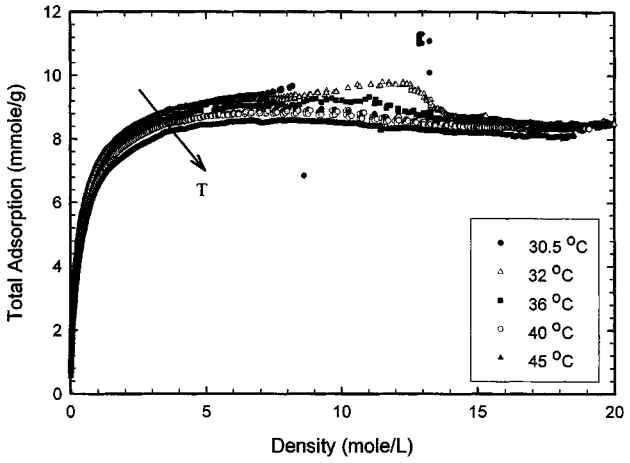


**Figure 6. Total adsorption of $CO_2$ on GAC based on the assumption of a constant volume of the adsorbed phase (0.36 $cm^3/g$).**

This seems to suggest that while the high-density behavior provides a reasonable value of $V^{ads}$ and $\rho^{ads}$, these values may not be constant over the entire pressure range.

In the region close to the critical point the total adsorption shows a significant maximum corresponding to the nonlinear portion in Figure 5. The calculated density in this region based on the assumption of a constant adsorbed phase volume is greater than that corresponding to close-packed $CO_2$ molecules. This suggests either that the molecules near the activated carbon surface are greatly compressed to solid-like density or that the spatial range of the adsorbed phase increases near the critical point. The latter is more likely, that is, that the volume of the adsorbed phase is not constant in the near-critical region. This is in agreement with theoretical predictions of multilayer adsorption near the critical point (Aranovich and Donohue, 1997b) and inferences reported by Specovius and Findenegg (1980) for the near-critical adsorption of ethylene on graphitized carbon black. Parallels have also been drawn between adsorption of supercritical fluids and the phenomenon of local density enhancements around solute molecules in supercritical fluid solutions (Subramanian et al., 1995). On the adsorbent surface one can envision a transition from a layer-filling mechanism to a multilayering or dynamic clustering phenomenon in the adsorbed phase as the critical point is approached. This transition begins well below the bulk critical density and in this aspect is similar to the enhanced density or charisma (Eckert and Knutson, 1993) of SCFs around spectroscopic probes (Brennecke et al., 1990).

Since this phenomenon occurs in the region where compressibility is very high, the accuracy of the EOS used to calculate bulk density (and buoyancy correction) is very important. The MBWR EOS (Jacobsen and Stewart, 1973; Ely et al., 1989) used in this study is also currently used in the NIST standard reference database (Lemmon et al., 2000) and compares well with other highly precise equations of state for $CO_2$ (Span and Wagner, 1996). The maximum calculated difference between the MBWR and the Span and Wagner isotherm was 5% (at 32°C and 7.4 MPa). In addition, precise control over temperature and pressure is also important; with a $\pm 0.05$°C and $\pm 1$-psi certainty in measurements of temperature and pressure, the resulting uncertainty in the density calculation at 32°C is 6%. This translates to an overall maximum uncertainty of 0.2% due to buoyancy corrections in the near-critical region. Thus, uncertainties in measurement and calculation cannot account for this enhanced adsorption in the near-critical region.

In a practical sense, this phenomenon would certainly be expected to affect the adsorption or desorption of solutes to or from the surface through increased competition for adsorption sites or increased localized solvent power. One could also hypothesize an effect on surface diffusion rates in supercritical extraction, adsorptive separations, or on reactant surface concentrations in heterogeneous catalysis.

### *Heat of adsorption*

The isosteric heat of adsorption ($q_{st}$) can be calculated from total adsorption isotherms as (Valenzuela and Myers, 1989)

$$q_{st} = RT^2\left[\frac{\partial \ln P}{\partial T}\right]_{\Gamma^{total}} = -R\left[\frac{\partial \ln P}{\partial (1/T)}\right]_{\Gamma^{total}}, \qquad (5)$$

where the subscript stands for constant total adsorption. This would give the ''absolute'' isosteric heat as opposed to the ''excess'' isosteric heat obtained from excess adsorption isotherms (Myers et al., 1997; Salem et al., 1998). The excess isosteric heat of adsorption in the near-supercritical region would be ambiguous due to the crossover of the excess adsorption isotherms. The near-continuous adsorption isotherms allow for the accurate calculation of the heat of adsorption at increasing coverage without the incorporation of an adsorption model or a polynomial fit. The heat of adsorption has to be calculated based on the total adsorption, and thus includes the assumption regarding the adsorbed phase volume. Figure 7 shows the isosteric heat of adsorption vs. molar coverage at several discrete points. Both the shape

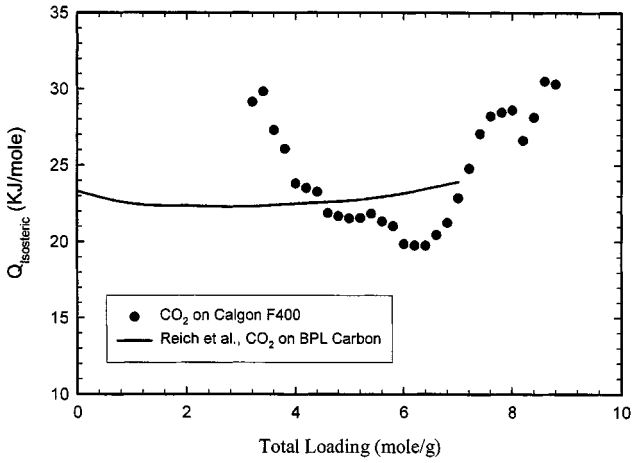


**Figure 7. Isosteric heat of adsorption calculated from experimental points based on total adsorption vs. data from Reich et al. (1980) based on Toth Isotherm fits to excess adsorption isotherms.**
Both are for similar, bituminous-based carbons.

and the magnitude agree well with previously published data for a similar activated carbon (Reich et al., 1980).

### *Two-dimensional equation of state model*

Two-dimensional equation-of-state (EOS) models for adsorption are based on the concepts developed by Gibbs and de Boer (de Boer, 1953; Ross and Olivier, 1971), which suggest that the adsorbed fluid can be visualized as a two-dimensional phase. This approach has been used by several researchers (Hoori and Prauznitz, 1967; Payne et al., 1968; DeGance, 1992; Zhou et al., 1994) for microporous adsorbents. In this article we have used the 2-D Peng-Robinson EOS, which is similar in form to the 3-D PR EOS, with the exceptions that pressure is replaced by a 2-D spreading pressure ($\pi$) and molar volume is replaced by a specific molar area ($A/\omega$, area per moles adsorbed). We have followed the development of Zhou et al. (1994):

$$A\pi + \frac{\alpha\omega^2}{1+2\beta\omega-(\beta\omega)^2}(1-\beta\omega) = \omega RT, \qquad (6)$$

where $\alpha$ and $\beta$ are analogous to the 3-D $a$ and $b$, respectively. It must be noted that the adsorbed amount, $\omega$, represents the "total" moles per unit area and not the excess, as measured experimentally. Thus, it is necessary to use an additional model as described in the previous section, describing the volume or the density of the adsorbed phase in order to determine the total adsorption from the excess.

The adsorbed phase represents an open system in equilibrium with the bulk fluid:

$$\mu^a = \mu^f \quad \text{and} \quad d\mu^a = d\mu^f. \qquad (7)$$

The chemical potentials ($\mu$) can be written in terms of fugacity ($f$) to give a relationship between the bulk and adsorbed phase properties:

$$Af^a = A\pi\phi^a = kRTf^f, \qquad (8)$$

where $k$ is the slope of the isotherm approaching the origin. The fluid-phase fugacity can be determined from an accurate EOS for the bulk-phase properties; we have used a modified BWR EOS (Jacobsen and Stewart, 1973; Ely et al., 1989). The adsorbed phase fugacity is obtained from the 2-D EOS (Eq. 6), resulting in the following final expression:

$$\ln f^f = \frac{\beta\omega}{1-\beta\omega} - \ln(1-\beta\omega) + \frac{\alpha\omega}{RT\left[1+2\beta\omega-(\beta\omega)^2\right]} + \frac{\alpha}{RT\beta\sqrt{8}}\ln\left[\frac{1+\left(1+\sqrt{2}\right)\beta\omega}{1+\left(1-\sqrt{2}\right)\beta\omega}\right] - \ln k. \qquad (9)$$

Although $A$ and $\pi$ are required in the development of the model (both these quantities cannot be directly measured for heterogeneous microporous materials), they are not present in the final form and their measurement/quantification is not required. Thus we obtain a model with three parameters $\alpha$, $\beta$, and $k$. Of these, $k$ can be estimated from low-pressure adsorption data as the slope of the isotherm at zero adsorption. In the absence of low-pressure data $k$ can also be determined as a third parameter. We have used a Fortran program to estimate the parameters to fit 2D-EOS to the data presented in the previous section; $k$ was determined by extrapolating low-pressure data. The effect of temperature on the fitted values of $\alpha$ was found to be minimal in the temperature range of our experiments; therefore, a constant av-

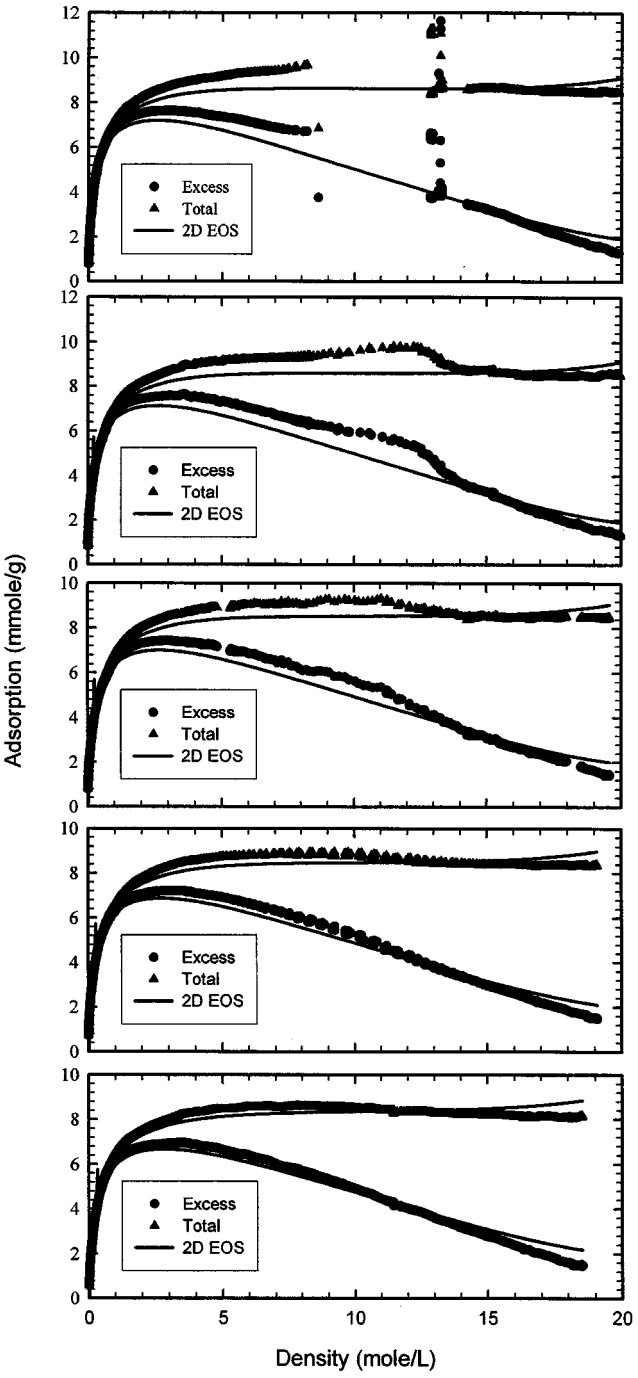


**Figure 8. 2-D–PR EOS model fits to data at (a) 30.5, (b) 32, (c) 36, (d) 40, (e) 45°C.**

**Table 2. Parameters Used in the 2D-PR EOS**

| $T$ (°C) | $\alpha$ (MPa·m$^3$·g/mmol) | $\beta$ (g/mmol) | ln $k$ |
|---|---|---|---|
| 30.5 | −178 | 0.0250 | 1.44 |
| 32 | −178 | 0.0254 | 1.16 |
| 36 | −178 | 0.0262 | 0.94 |
| 40 | −178 | 0.0270 | 0.71 |
| 45 | −178 | 0.0280 | 0.49 |

erage value was chosen while $\beta$ was varied. Figure 8 shows the model fits for the five temperatures. Table 2 shows the values of the fitted parameters used.

The 2D-EOS is able to describe the adsorption behavior qualitatively over the broad pressure–density range. However, due to the enhanced adsorption phenomenon in the near-critical region, it cannot catch the shape of the adsorption isotherms at temperatures closer to the critical point. While such a model based on a 2-D adsorbed phase is inherently incapable of predicting the complex adsorption behavior in the near-critical region, its usefulness lies in its flexibility when dealing with multicomponent systems where single-phase properties can be used in conjunction with appropriate mixing rules. A truly quantitative model for this system would need to be based on a realistic theory for the density profile and would take into account the inhomogeneous nature of the adsorbed phase properties in the near-critical region.

## Conclusions

We have presented precise, high-resolution data for the adsorption of $CO_2$, commonly used as a supercritical solvent in various processes. The near continuous data allow for detailed thermodynamic analysis and will aid in the development of modeling techniques to describe the adsorption behavior. Adsorption data in the near-critical region suggests that the adsorbed phase undergoes a reversible transition from layer filling to clustering very near the solvent's critical point and back to layer filling as the critical pressure is exceeded. At high densities, the adsorbed phase volume and density become constant and relatively insensitive to temperature. Knowledge of the adsorption behavior of the pure supercritical solvent will aid in the understanding of single- and multiple-solute adsorption–desorption behavior in supercritical fluids, which is intrinsic to their successful application in heterogeneous separation and reaction processes.

## Acknowledgment

The authors gratefully acknowledge the financial support provided for this work by the National Science Foundation through Grants CTS-9409786 and EEC-9815677, and by the donors of The Petroleum Research Fund, administered by the American Chemical Society. We thank Dr. Bhavik Bakshi and Mohammed Nounou for their help with the data rectification and noise reduction, and Dr. David Bush for sharing his $CO_2$ equation of state program.

## Literature Cited

Afrane, G., and E. H. Chimowitz, "A Molecular Thermodynamic Model for Adsorption Equilibria from Supercritical Fluids," *J. Supercrit. Fluids*, **6**, 143 (1993).

Aranovich, G. L., and M. D. Donohue, "Adsorption of Supercritical Fluids," *J. Colloid Int. Sci.*, **180**, 537 (1996).

Aranovich, G. L., and M. D. Donohue, "Determining Surface Areas from Linear Adsorption Isotherms at Supercritical Conditions," *J. Colloid Interface Sci.*, **194**, 392 (1997a).

Aranovich, G. L., and M. D. Donohue, "Predictions of Multilayer Adsorption Using Lattice Theory," *J. Colloid Interface Sci.*, **189**, 101 (1997b).

Bakshi, B. R., P. Bansal, and M. N. Nounou, "Multiscale Rectification of Random Errors Without Fundamental Process Models," *AIChE J.*, **45**, 1041 (1997).

Brennecke, J. F., and C. A. Eckert, "Phase Equilibria for Supercritical Fluid Process Design," *AIChE J.*, **35**, 1409 (1989).

Brennecke, J. F., D. L. Tomasko, J. Peshkin, and C. A. Eckert, "Fluorescence Spectroscopy Studies in Dilute Supercritical Solutions," *Ind. Eng. Chem. Res.*, **29**, 1682 (1990).

Chen, J. S., D. S. H. Wong, C. S. Tan, R. Subramanian, C. T. Lira, and M. Orth, "Adsorption and Desorption of Carbon Dioxide onto and from Activated Carbon at High Pressures," *Ind. Eng. Chem. Res.*, **36**, 2808 (1997).

DeBoer, J. H., *The Dynamic Character of Adsorption*, Clarendon Press, Oxford (1953).

DeGance, A. E., "Multicomponent High-Pressure Adsorption Equilibria on Carbon Substrates: Theory and Data," *Fluid Phase Equilibria*, **78**, 99 (1992).

Donoho, D. L., I. M. Johnstone, G. Kerkyacharian, and D. Picard, "Wavelet Shrinkage: Asymptotia?" *J. Royal Stat. Soc. B*, **57**, 301 (1995).

Eckert, C. A., and B. L. Knutson, "Molecular Charisma in Supercritical Fluids," *Fluid Phase Equilibria*, **83**, 93 (1993).

Ely, J. F., W. M. Haynes, and B. C. Bain, "Isocharic (P, Vm, T) Measurements on $CO_2$ and on (0.982 $CO_2$ + 0.018 $N_2$) from 250 to 330 K at Pressures to 35 Mpa," *J. Chem. Thermodynamics*, **21**, 879 (1989).

Findenegg, G. H., "High Pressure Adsorption of Gases on Homogeneous Surfaces," *Fundamentals of Adsorption*, A. L. Myer and G. Belford, Engineering Foundation, New York (1983).

Gregg, S. J., and K. S. W. Sing, *Adsorption, Surface Area and Porosity*, Academic Press, London (1967).

Gubbins, K. E., "Theory and Simulation of Adsorption in Micropores," *Physical Adsorption: Experiment, Theory and Applications*, J. Fraissard and C. W. Conner, eds., Kluwer, Dordrecht, The Netherlands (1997).

Haydel, J. J., and R. Kobayashi, "Adsorption Equilibria in the Methane-Propane-Silica Gel System," *Ind. Eng. Chem. Fundam.*, **6**, 546 (1967).

Haydel, J. J., and R. Kobayashi, "Adsorption Equilibria in the Methane-Propane-Silica Gel System at High Pressures," *Ind. Eng. Chem. Fundam.*, **6**, 546 (1968).

Hoori, S. E., and J. M. Prauznitz, "Monolayer Adsorption of Gas Mixtures on Homogeneous and Heterogeneous Solids," *Chem. Eng. Sci.*, **22**, 1025 (1967).

Jacobsen, R. T., and R. B. Stewart, "Thermodynamic Properties of Nitrogen Including Liquid and Vapor Phases from 63 K to 2000 K with Pressures to 10,000 bar," *J. Phys. Chem. Ref. Data*, **2**, 757, (1973).

Johnston, K. P., D. G. Peck, and S. Kim, "Modeling Supercritical Mixtures—How Predictive Is It? *Ind. Eng. Chem. Res.*, **28**, 1115 (1989).

Jones, W. M., P. J. Isaac, and D. Phillips, "The Adsorption of Carbon Dioxide and Nitrogen by Porous Plugs of Lamp Black," *Trans. Faraday Soc.*, **55**, 1953 (1959).

Jwayyed, A. M., R. Humayun, and D. L. Tomasko, "High Pressure Flow Gravimetric Apparatus for Supercritical Fluid Extraction Studies," *Rev. Sci. Instrum.*, **68**, 4542 (1997).

Kikik, I., P. Alessi, A. Cortesi, S. J. Macnaughton, N. R. Foster, and B. Spika, "An Experimental Study of Supercritical Adsorption Equilibria of Salicyclic Acid on Activated Carbon," *Fluid Phase Equilibria*, **117**, 304 (1996).

King, J. W., "Supercritical Fluid Interaction at the Gas-Solid Interface," *ACS Symp. Ser.*, Washington, DC, 150 (1987).

Lemmon, E. W., M. O. McLinden, and D. G. Friend, *NIST Chemistry WebBook, NIST Standard Reference Database Number 69*, NIST, Gaithersburg, MD (2000).

Machin, W. D., ''Properties of Three Capillary Fluids in the Critical Region,'' *Langmuir*, **15**, 169 (1999).
McHugh, M., and V. Krukonis, *Supercritical Fluid Extraction: Principles and Practice*, Butterworth-Heinemann, Boston (1993).
Menon, P. G., ''Adsorption at High Pressures,'' *Chem. Rev.*, **68**, 277 (1968).
Michalski, T., A. Benini, and G. H. Findenegg, ''A Study of Multilayer Adsorption and Pore Condensation of Pure Fluids in Graphite Substrates on Approaching the Bulk Critical Point,'' *Langmuir*, **7**, 185 (1991).
Morishige, K., and M. Shikimi, ''Adsorption Hysteresis and Pore Critical Temperature in a Single Cylindrical Pore,'' *J. Chem. Phys.*, **108**, 7821 (1998).
Myers, A. L., J. A. Callus, and G. Calleja, ''Comparison of Molecular Simulation of Adsorption with Experiment,'' *Adsorption*, **3**, 107 (1997).
O'Brien, J. A., T. W. Randolph, C. Carlier, and S. Ganapathy, ''Quansicritical Behavior of Dense-Gas Solvent-Solute Clusters at Near-Infinite Dilution,'' *AIChE J.*, **39**, 1061 (1993).
Ozawa, S., S. Kusumi, and Y. Ogino, ''High Pressure Adsorption of Carbon Dioxide on Several Activated Carbons with Different Pore Size Distribution,'' *Int. Conf. High Pressure*, Physical-Chemical Society of Japan, Tokyo (1975).
Payne, H. K., G. A. Sturdevant, and T. W. Lealand, ''Improved Two-Dimensional Equation of State to Predict Adsorption of Pure and Mixed Hydrocarbons,'' *Ind. Eng. Chem. Fundam.*, **7**, 363 (1968).
Reich, R., W. T. Ziegler, and W. A. Rogers, ''Adsorption of Methane, Ethane, and Ethylene Gases and their Binary and Ternary Mixtures and Carbon Dioxide on Activated Cargon at 212-301 K and Pressures to 35 Atmospheres,'' *Ind. Eng. Chem. Process Des. Dev.*, **19**, 336 (1980).
Ross, S., and J. P. Olivier, *On Physical Adsorption*, Interscience, New York (1971).
Sahle-Demessie, E., K. L. Levien, and J. L. Morrell, ''Impregnating Porous Solids Using Supercritical $CO_2$,'' *Chemtech*, **28**, 12 (1998).
Salem, M. M. K., P. Braeuer, M. V. Szombathely, M. Heuchel, P. Harting, K. Quitzch, and M. Jaroniec, ''Thermodynamics of High-Pressure Adsorption of Argon, Nitrogen, and Methane on Microporous Adsorbents,'' *Langmuir*, **14**, 3376 (1998).
Sircar, S., ''Gibbsian Surface Excess for Gas Adsorption,'' *Ind. Eng. Chem. Res.*, **38**, 3670 (1999).
Sircar, S., and A. L. Myers, ''Adsorption from Liquid Mixtures from Solids: Thermodynamics of Excess Properties and Their Temperature Coefficients,'' *Adsorp. Technol.*, **67**, 11 (1971).
Span, R., and W. Wagner, ''A New Equation of State for Carbon Dioxide Covering the Region from the Triple-Point Temperature to 1100 K at Pressures up to 800 MPa,'' *J. Phys. Chem. Ref. Data*, **25**, 1509 (1996).
Specovius, J., and G. H. Findenegg, ''Study of a Fluid Solid Interface over a Wide Density Range Including the Critical Region. I. Surface Excess of Ethylene/Graphite,'' *Ber. Bunsenges. Phys. Chem.*, **84**, 690 (1980).
Strubinger, J. R., and J. F. Parcher, ''Surface Excess (Gibbs) Adsorption Isotherms of Supercritical Carbon Dioxide on Octadecyl Bonded Silica Stationary Phases,'' *Anal. Chem.*, **61**, 951 (1989).
Subramanian, R., H. Pyada, and C. T. Lira, ''An Engineering Model for Adsorption of Gases onto Flat Surfaces and Clustering in Supercritical Fluids,'' *Ind. Eng. Chem. Res.*, **34**, 3830 (1995).
Tan, C. S., and D. C. Liou, ''Adsorption Equilibrium of Toluene from Supercritical Carbon Dioxide on Activated Carbon,'' *Ind. Eng. Chem. Res.*, **29**, 1412 (1990).
Thommes, M., G. H. Findenegg, and H. Lewandowski, ''Critical Adsorption of sf6 on a Finely Divided Graphite Substrate,'' *Ber. Bunsenges. Phys. Chem.*, **98**, 477 (1994).
Tucker, S. C., and M. W. Maddox, ''The Effect of Solvent Density Inhomogeneities on Solute Dynamics in Supercritical Fluids: A Theoretical Perspective,'' *J. Phys. Chem. B*, **102**, 2437 (1998).
Valenzuela, D. P., and A. L. Myers, *Adsorption Equilibria Data Handbook*, Prentice Hall, Englewood Cliffs, NJ (1989).
Wakasugi, Y., S. Ozawa, and Y. Ogino, ''Physical Adsorption of Gases at High Pressure,'' *J. Colloid Interface Sci.*, **79**, 399 (1981).
Weireld, G. D., M. Frere, and R. Jadot, ''Automated Determination of High-Temperature and High-Pressure Gas Adsorption Isotherms Using a Magnetic Suspension Balance,'' *Meas. Sci. Technol.*, **10**, 117 (1999).
Zhou, C., F. Hall, K. Gasem, A. M., and R. L. Robinson, Jr., ''Predicting Gas Adsorption Using Two-Dimensional Equations of State,'' *Ind. Eng. Chem. Res.*, **33**, 1280 (1994).

*Manuscript received Nov. 1, 1999, and revision received Mar. 27, 2000.*